https://doi.org/10.5194/nhess-2021-13
Preprint. Discussion started: 11 February 2021

Natural Hazards and Earth System Sciences
Discussions

Global ground strike point characteristics in negative downward lightning flashes — part 2: Algorithm validation

Dieter R. Poelman[1], Wolfgang Schulz[2], Stephane Pedeboy[3], Leandro Z. S. Campos[4], Michihiro Matsui[5], Dustin Hill[6], Marcelo Saba[7], Hugh Hunt[8]

[1]Royal Meteorological Institute, Brussels, Belgium
[2]Austrian Lightning Detection and Information System (ALDIS), Vienna, Austria
[3]Météorage, Pau, France
[4]Campos Scientific Computing
[5]Franklin Japan Corporation, Sagamihara 212-0212, Japan
[6]Scientific Lightning Solutions LLC (SLS), Titusville, Florida, USA
[7]National Institute for Space Research, INPE, São José dos Campos, Brazil
[8]The Johannesburg Lightning Research Laboratory, School of Electrical and Information Engineering, University of Witwatersrand Johannesburg, Johannesburg, South Africa

Correspondence to: Dieter R. Poelman (dieter.poelman@meteo.be)

Abstract. At present the lightning flash density is a key input parameter to assess the risk of occurrence of a lightning strike in a particular region of interest. Since it is known that flashes tend to have more than one ground termination point on average, the use of ground strike point densities as opposed to flash densities is more appropriate. Lightning location systems (LLSs) do not directly provide ground strike point densities. However, ingesting their observations into an algorithm that groups strokes in respective ground strike points results in the sought after density value. The aim of this study is to assess the ability of three distinct ground strike point algorithms to correctly determine the observed ground-truth strike points. The output of the algorithms is tested against a large set of ground-truth observations taken from different regions around the world, including Austria, Brazil, France, Spain, South Africa and the United States of America. These observations are linked to the observations made by local LLSs in order to retrieve the necessary parameters of each lightning discharge and serves as inputs for the algorithms. It follows that all three of the algorithms perform well, with success rates up to about 90% to retrieve the correct type of the strokes in the flash, i.e., whether the stroke creates a new termination point or follows a pre-existing channel. The most important factor that influences the algorithms' performance is the accuracy by which the strokes are located by the LLS. Additionally, it is shown that the strokes' peak current plays an important role, whereby strokes with a larger absolute peak current have a higher probability of being correctly classified compared to the weaker strokes.

https://doi.org/10.5194/nhess-2021-13
Preprint. Discussion started: 11 February 2021


Natural Hazards and Earth System Sciences Discussions

1 Introduction

Severe weather has always been around. However, its global impact on both society and economies increases steadily, with no signs of decline whatsoever towards the future. More specifically, the deleterious effects of lightning discharges cannot be underestimated. In this respect, cloud-to-ground (CG) flashes play a particular part since they have an enormous impact on human safety, both directly and indirectly. Besides lightning-caused fatalities and injuries that are reported each year worldwide (Curran et al. 2000; Holle et al. 2005, 2016), it is a well-known fact that lightning is a major cause of, for example, wildfires when the conditions to ignite fire near the vicinity of the ground strike point are fulfilled (Balch et al., 2017; Williams, 2016; Schultz et al., 2019). On the other hand, the economic effects of lightning damage to property are immense, whether being an individual household or a large-sized company, with total costs that quickly can spiral out of control. In this matter, electrical appliances are vulnerable to the electromagnetic fields induced by lightning. Additionally, the search for alternative ways of generating energy has led to the construction of vast amounts of wind turbines and wind and solar farms all over the world, to name but one other example. However, it has been demonstrated by Montanyà et al. (2014) by analyzing LMA observations in Spain that the rotating blades of wind turbines can trigger lightning, thereby causing self-induced damages. Not to mention the detrimental effects of lightning in other areas such as aviation, it is clear that adequate lightning protection measures need to be put at place to mitigate the effects of lightning impacts. For a comprehensive overview of lightning hazards to human societies the interested reader is referred to Yair (2018).

Over the years, our knowledge of thunderstorms has greatly improved, not least in the field of lightning. By means of high-speed cameras, it has been observed that roughly half of the downward negative CG multiple stroke flashes exhibit more than one ground strike point (GSP). With an average value varying around 1.5 to 1.7 GSPs per flash (Rakov et al., 1994; Hermant, 2000; Valine and Krider, 2002; Saraiva et al., 2010, Poelman et al., 2021 companion paper). This implies that the average number of lightning strike points is about 70% higher than the observed number of flashes. Additionally, the distance between the different GSPs and the first stroke in the flash is of the order of a few kilometers (Thottappillil et al., 1992; Valine et al., 2002; Stall et al., 2009). It follows that every ground strike point is a potential threat and therefore ground strike points ought to be taken into account when it comes to lightning risk estimation for lightning protection.

Nowadays the primary input parameter in lightning risk assessment applications is the lightning flash density, N_G. The latter is defined as the number of CG flashes per square kilometer per year. In the past, an empirical formula was applied to relate N_G to the keraunic level of thunderstorm days. However, progress made over the years to detect lightning discharges by means of lightning location systems (LLSs) has led to N_G being determined from the ground flash measurements by LLSs. By definition, the location of a flash is determined by that of the first stroke in the flash. Taking into account that, on average more than one GSP is observed per flash, it follows that the use of N_G in the risk calculation of lightning protection leads to an underestimation of the hazard. It is for this reason that N_G should be replaced by the lightning strike point density N_{SG}. Nowadays LLSs provide stroke locations with median accuracies in the order of a few hundred meters or better, hence LLSs can provide N_{SG} after applying a dedicated algorithm to group the individual strokes within a flash in ground strike points.

https://doi.org/10.5194/nhess-2021-13
Preprint. Discussion started: 11 February 2021


Natural Hazards and Earth System Sciences Discussions

In this study, three different ground strike point algorithms are tested against a large set of high-speed video measurement data from multiple regions to find out their ability to determine the observed ground strike points correctly. In Sections 2 and 3 the different lightning location systems and ground-truth data sets are described, respectively, followed by the characteristics of the algorithms in Section 4. In Section 5 the results are discussed, while Section 6 summarizes the study and draws some further conclusions.

2. Lightning Location Systems involved

The ground-truth data sets outlined in Poelman et al. (2021, companion paper) and gathered in Austria (AT), Brazil (BR), South-Africa (SA), and the United States of America (US), serve among others as input for the ground strike point algorithms described further in Sec. 3. In addition, two extra ground-truth data sets collected in France (FR) and Spain (ES) are included in this study. In order to retrieve information regarding location, peak current and semi-major axis, the ground truth data sets are linked to the observations made by a local ground-based LLS. In this Section, the different LLSs are briefly described.

2.1. OVE-ALDIS

ALDIS operates a sensor network of eight low frequency (LF) lightning detection sensors in Austria while the central processor ingests additional sensors from neighbouring countries. In addition, ALDIS is partly known for its continuous work related to the European Cooperation for Lightning Detection (EUCLID); recognized as one of the best documented networks in Europe in terms of location accuracy (LA) and detection efficiency (DE) estimates. This is made possible partly due to the observations made at the instrumented Gaisberg Tower in Austria and supplemented by mobile video and field recording system (VFRS) observations in Austria, as well as throughout Europe. Due to continuous adaptation and improvement of the system with on-going hard- and software upgrades, the median LA is in the range of 100 m (for more detailed information see Schulz et al., 2016; Poelman et al., 2016; Diendorfer, 2016).

2.2. Météorage

The French national LLS has been operated by Météorage (MTRG) since 1986. It detects low-frequency electromagnetic signals generated by CG lightning, as well as a fraction of large amplitude CC discharges much in the same way as ALDIS. In the beginning, the LLS was made up of sensors placed only in France. Over the years this core network expanded with compatible sensors of neighboring partners, providing seamless extended observation coverage over western Europe. In this study, the LLS of MTRG is used to match the ground-truth observations taken in France and Spain. Similar DE and LA values as the ones stated above for OVE-ALDIS are applicable for this network.

https://doi.org/10.5194/nhess-2021-13
Preprint. Discussion started: 11 February 2021


Natural Hazards and Earth System Sciences Discussions

2.3. RINDAT

At the time, the ground-truth observations used in this work were carried out, the Brazilian Lightning Detection Network (RINDAT) was composed out of a mix of 47 sensors. The network has evolved somewhat since then resulting in an improved network performance. Nevertheless, a stroke and flash DE of RINDAT of respectively of 55% and 87% was reported by Ballarotti et al. (2006). Additionally, an upper limit on the LA was retrieved of about 5 km. More information on the characteristics of the network is given by Naccarato and Pinto [2009].

2.4. SALDN

The South African Lightning Detection Network (SALDN) was first installed in South Africa in 2006 by the South African Weather Services (SAWS), originally consisting of 19 Vaisala LS7000 sensors spread across the country. The network has since been upgraded to 24 sensors across the country with an average sensor baseline of approximately 150 km, forming a grid across the country (Gijben, 2012; Evert, 2017). Self-evaluation of the network estimates detection efficiencies above 90 % and location accuracies within 500 m for all of the coverage of the country, only dropping below these levels at the borders (of the country and the network). Ground-truth evaluations report downward event detection efficiencies of 85-90 %. These evaluations further indicate a median location error within 150 m (Hunt, 2014, Fensham, 2018, Hunt, 2020).

2.5. NLDN

The U.S. national lightning detection network (NLDN) adopts a combination of time-of-arrival and direction finding technology (Cummins and Murphy 2009), similar to the other networks, to geolocate lightning CG strokes and IC pulses since 1989. The Contiguous United States (CONUS) is covered by approximately 100 LS7002 sensors (Nag et al., 2014). The detection efficiency and location accuracy of the NLDN has been evaluated thoroughly using video observations (Biagi et al. 2007; Cummins et al. 2014; Zhang et al. 2015), tower data (Lafkovici et al. 2006; Cramer and Cummins 2014) and triggered lightning data (Jerauld et al. 2005; Nag et al. 2011; Mallick et al. 2014). It follows that the flash DE is expected to be in the order of 95% within CONUS. The location accuracy is approximately 150 to 250 m over the majority of the United States, and decreasing somewhat to 250-500 m toward the edges of the network.

3. Data sets

Since not all of the strokes observed by the high-speed cameras and electric field mills were detected by the different LLSs, the data sets used in this study differ slightly from the ones presented in Poelman et al. (2021, companion paper). Note that the list of flashes to test the performance of the ground strike point algorithms is additionally enlarged by two extra data sets gathered in France and Spain. The quality of the latter two data sets is of the same level as compared to the data sets introduced in Poelman et al. (2021, companion paper). However, the limited video recording time of 500 ms prohibits its use in Poelman et al. (2021, companion paper). Note that a flash is completely removed if a stroke that creates a new GSP is not

https://doi.org/10.5194/nhess-2021-13
Preprint. Discussion started: 11 February 2021

Natural Hazards and Earth System Sciences Discussions

Table 1. Data set characteristics for Austria (AT), Brazil (BR), France (FR), South Africa (SA), Spain (ES) and the United States of America (US)

Parameter	LLS					
	AT	*BR*	*FR*	*SA*	*ES*	*US*
N(flashes)	474	111	354	392	76	73
N(strokes)	1373	385	894	1174	183	273
N(GSP)	808	191	585	508	121	114
Location Accuracy						
Sample Size	582	210	325	689	63	161
Mean (km)	0.38	1.88	0.73	0.65	0.37	0.67
Median (km)	0.11	1.0	0.19	0.11	0.11	0.13
95th percentile (km)	1.76	6.74	3.82	2.06	1.43	4.15
Semi-major Axis						
Mean (km)	0.31	0.69	0.30	0.36	0.17	0.43
Median (km)	0.08	0.50	0.20	0.20	0.15	0.20
95th percentile (km)	1.43	1.66	0.80	1.50	0.33	1.10
Resolution provided by LLS (m)	2012: 100 2015-2018: 10	100	2013-2015: 100 2016: 10	100	10	100
Median absolute peak current (kA)						
1st strokes	12.4	19.7	15.6	18.0	11.9	31.4
Subsequent strokes	10.1	15.4	13.3	13.0	11.2	16.4
NGC	12.4	18.8	14.7	18.0	11.5	27.5
PEC	8.3	14.8	12.8	12.0	11.3	14.3
Distance between GSP and 1st stroke in the flash						
Sample size	335	84	235	116	46	43
Mean (km)	2.53	5.12	2.67	3.79	2.80	1.66
Median (km)	2.08	3.0	2.21	2.36	2.46	1.46
95th percentile (km)	5.92	7.43	6.73	13.38	5.5	3.81
Maximum (km)	25.4	42.7	13.6	20.8	6.7	5.8

https://doi.org/10.5194/nhess-2021-13
Preprint. Discussion started: 11 February 2021


Natural Hazards and Earth System Sciences Discussions

detected by the LLS since this would impact the success rate of the algorithm further described in Section 4. In what follows, some of the characteristics of the reduced data sets are discussed. Note that detection efficiency projections of the LLS are out of the scope of this study and therefore detailed investigation is disregarded as such. Nevertheless, one can find in the references for the individual LLS detection efficiency estimations of the individual networks.

Some of the characteristics that can play a role in the further course of the study are listed in Table 1 for the different data sets. The combined data sets include a total of 1480 flashes, consisting of 4282 strokes, whereby a total of 2327 ground strike points are distributed among them. The size of the data sets, in terms of flashes, strokes and ground strike points, are somewhat smaller compared to Poelman et al. (2021, companion paper) for the reason described above. Because of this, it is not possible and not valid to use the numbers given in Table 1 for detection efficiency estimations.

The LA of the different LLS can be quantified by using the strokes that follow the same channel as observed from the consecutive high-speed images. Since those strokes are assumed to strike ground at the same point, the differences between the stroke positions within a GSP lead to the LA estimation after applying a downscaling factor of $\sqrt{2}$. The latter scaling is applied since both positions are subject to random errors, by analogy of Schulz et al. (2010) and Biagi et al. (2007). The differences determined by this method should be regarded as upper bounds of the actual position differences because there is the possibility that the channel geometry and/or the actual ground contact varied slightly from stroke to stroke and was not resolved by the camera. The results hereof can be consulted in Table 1. All of the LLSs have median LA in the range of 0.11-0.19 km, except for Brazil with a median LA of 1 km. These LA values correspond with previous LA estimates in other studies mentioned in Section 2 for the individual networks.

An alternative way to look at the location quality is to monitor the semi-major axis (SMA) of the error ellipse within which there is 50% probability that the stroke actually attached. From Table 1, it follows that the SMA for BR is highest, indicating that the location quality is lower compared to the other data sets. It also confirms the LA values retrieved by the method described above.

Estimated (measured) median peak current values for 1st strokes, subsequent strokes, NGCs and PECs are also presented in Table 1. As expected, the 1st strokes exhibit higher (absolute) peak currents compared to the subsequent strokes, analogue to the peak current values of NGCs versus PECs. Since higher peak current strokes tend to be detected on average by a larger amount of lightning sensors, the coordinates appointed by the LLS are likely to be of higher accuracy compared to strokes exhibiting a lower peak current. This may influence the probability of the algorithms to distinguish correctly between a new GSP or a PEC, as will be discussed later on.

Finally, values for the distance between the first stroke in the flash, i.e., 1st GSP, and subsequent GSPs within the flash are illustrated in Table 1 as well. Median values vary between 1.46 km (US) and 3.0 km (BR). The retrieved distances agree well with those found in previous studies, e.g., Stall et al. (2009) and Thottappilil et al. (1992).

https://doi.org/10.5194/nhess-2021-13
Preprint. Discussion started: 11 February 2021


Natural Hazards and Earth System Sciences Discussions

4. Algorithms

The sole purpose of a ground strike point algorithm is to group the different strokes of a flash into one or more ground strike points. The ultimate goal is to mimic, as accurately as possible, the exact distribution of GSPs compared to what is observed in the high-speed camera images. The ability to do so enables the user to determine, with a high degree of certainty, on a predefined geographical and periodical scale, the ground strike point density based on a large set of actual LLS observations. To our knowledge, four such GSP algorithms exist to date. One of those has been described by Cummins et al. (2012). The empirical formulae that resulted from that analysis was based on LLS data employing IMPACT sensors. Since in this study, the LLSs described in Section 2 utilize so-called LS700x sensor technology of Vaisala (except for BR), it is believed that this particular method is unsuitable to be applied to the data in this study and is hence disregarded (Cummins, private communication). In what follows, the three remaining algorithms are described.

4.1. Algorithm 1 (A1)

Developed by MTRG, this iterative K-means method works as follows. During the first iteration, the first stroke in the flash is taken as the location of the first GSP. Then subsequent strokes are assigned to a GSP if and only if the distance falls within a pre-defined minimum geometrical distance threshold. If the distance between the stroke and the previously determined GSPs is greater than this threshold, the stroke creates a new GSP, otherwise it is assigned to the closest GSP. Before an iteration ends, the GSP positions are updated according to the mean locations of the strokes assigned to the GSP, whereby a weight is given to each stroke inversely proportional to the respective semi-major axis (SMA), i.e., strokes with smaller SMAs will influence the GSP location more than strokes with large SMAs. Then a new iteration can start and the process is repeated until the mean GSP positions do not vary anymore; meaning all the strokes are durably assigned to their ground contact. It is important to note that strokes with peak current $|I_p| < 6$kA and/or with SMA values above 2 km are assigned to the previous GSP regardless of their position. For further details on this algorithm, the interested reader is referred to Pedeboy et al. (2012).

4.2. Algorithm 2 (A2)

This iterative K-means method has been developed and described in great detail in Campos et al. (2015, 2016). As a first step, strokes are sorted into two main groups, i.e., those with low and those with high SMA values based on a user-defined threshold. Initially, the algorithm tries to group the strokes with low SMAs among themselves, thereby creating the first set of GSPs. To do so, the mean location among the low-SMA strokes is first calculated. Then the algorithm checks the distance between each low-SMA stroke and this mean location. The resulting distances are then compared against a so-called spherical threshold. This threshold depends on the properties of the strokes in the flash, defined as twice the maximum SMA value among the low-SMA strokes in the flash. If all distances fall below the spherical threshold, the low-SMA strokes are grouped within one GSP. However, in the case where one distance is larger and the rest are smaller than the threshold, a new

https://doi.org/10.5194/nhess-2021-13
Preprint. Discussion started: 11 February 2021


Natural Hazards and Earth System Sciences Discussions

iteration starts whereby now two potential GSP locations are tested. The first GSP adopts the location of the stroke in the previous iteration with the distance larger than the threshold, and the location of the second GSP is the mean of the locations of the other strokes. The algorithm repeatedly checks the distances up to the point that the greatest distance between a GSP and all its associated strokes is smaller than the threshold, implying that the low-SMA groups are grouped in a fixed set of GSPs. Subsequently, the algorithm attempts to group the strokes with high-SMA into the previous retrieved GSPs, according to an elliptical scaling method. In order to do so, the error ellipse is scaled until it intersects with the location of one of the GSPs. The scaling value indicates how many times the scaled ellipse is larger or smaller than the original error ellipse. A maximum elliptical scaling factor of two is adopted in this study. If the scaling factor is below two, then it is assigned to that GSP and not otherwise. Finally, the algorithm groups redundant GSPs if the distances are smaller than the threshold used to split strokes into strokes with low- and high-SMAs.

4.3. Algorithm 3 (A3)

The most recent method has been introduced by Matsui et al. (2019). This non-iterative approach excels in its simplicity whereby a stroke with a distance below a certain threshold is assigned to an existing GSP when the 50% probability ellipse overlaps with one or more of the other error ellipses of strokes already assigned to that GSP. The GSP location is updated directly as the mean of the locations of the strokes. If not, a new GSP is created and the distances of the subsequent strokes are tested against the locations of the pre-existing GSPs.

4.4. Some initial examples

The flashes displayed here are examples of real flashes from the data set of this study and are specifically chosen to explain the principles employed by the algorithms in an uncomplicated manner. Of course, more complicated flashes exist with higher multiplicities.

Figure 1a displays a two-stroke flash with the original error ellipses displayed as solid lines. The peak currents of the strokes are -11.3kA and -3.5kA respectively. The strokes are about 850 m apart and have SMA values of 400m and 1km respectively. A1 will always group the strokes together in one GSP irrespective of their distance, since the second stroke has an absolute peak current smaller than 6 kA. For A2, adopting a distance threshold of, e.g., 500m results in stroke 1 being the first GSP as it is the only low-SMA stroke in the flash. Stroke 2 is in this case regarded as a high-SMA and elliptical scaling is applied. The scaled error ellipse is displayed as the dotted ellipse in the plot. The error ellipse is scaled by a factor of less than 2 before it intersects with the location of the GSP. Therefore, these strokes will be grouped into one ground strike point. In the case of A3, the error ellipses overlap, therefore the grouping depends solely on the chosen distance threshold. If the threshold is below 850 m, then it will create two GSPs otherwise the strokes are grouped into a single GSP.

The composition of the four strokes from another flash is visualized in Fig. 1b. The first three have an SMA of 400m, while the fourth stroke has an SMA of 500 m. If a distance threshold of 200m is adopted, A1 will create four GSPs according, since the distances are all larger than 200 m for all combinations possible. If the threshold is increased to 1 km however, the

https://doi.org/10.5194/nhess-2021-13
Preprint. Discussion started: 11 February 2021

Natural Hazards and Earth System Sciences
Discussions

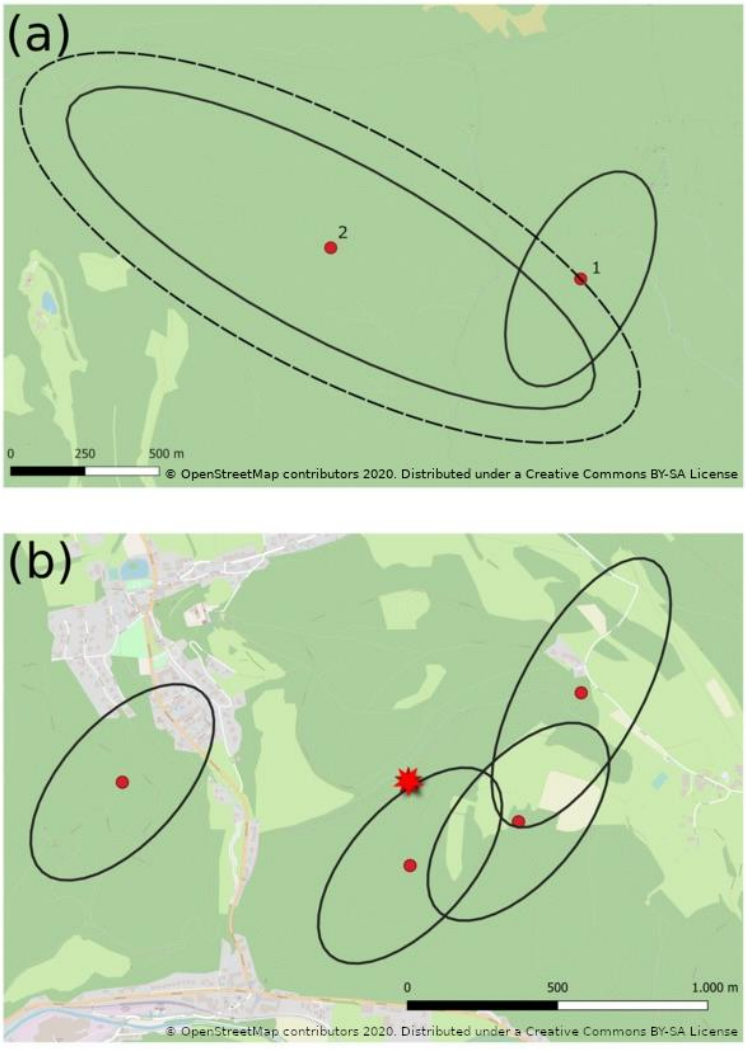

Figure 1: a) Example of a two-stroke flash. The original error ellipses are displayed (solid) alongside the scaled error ellipse of stroke 2 (dashed) as used by A2. b) A flash with multiplicity 4. The star denotes the average position of all four strokes.

algorithm results in one GSP. For A2, let's take a threshold of 200m to separate the low and high-SMA strokes. All strokes are considered as high-SMA events and therefore only elliptical scaling is applied. Since the error ellipses overlap already a lot, it is possible to envision that the scaling factors will be below 2 and therefore the last three strokes will be grouped into a single GSP, while the 1st stroke is a GSP on its own. When adopting 1 km as threshold, all strokes are considered as low-SMA strokes and only spherical grouping is applied. First, the mean location of all 4 strokes is calculated, highlighted by the star in the plot. Then the distances of the strokes to the star are calculated. Since the distances are all below 1 km, they are grouped into a single GSP. In the case of A3, the first stroke will always be a GSP on its own since the error ellipse does not

https://doi.org/10.5194/nhess-2021-13
Preprint. Discussion started: 11 February 2021

Natural Hazards and Earth System Sciences
Discussions

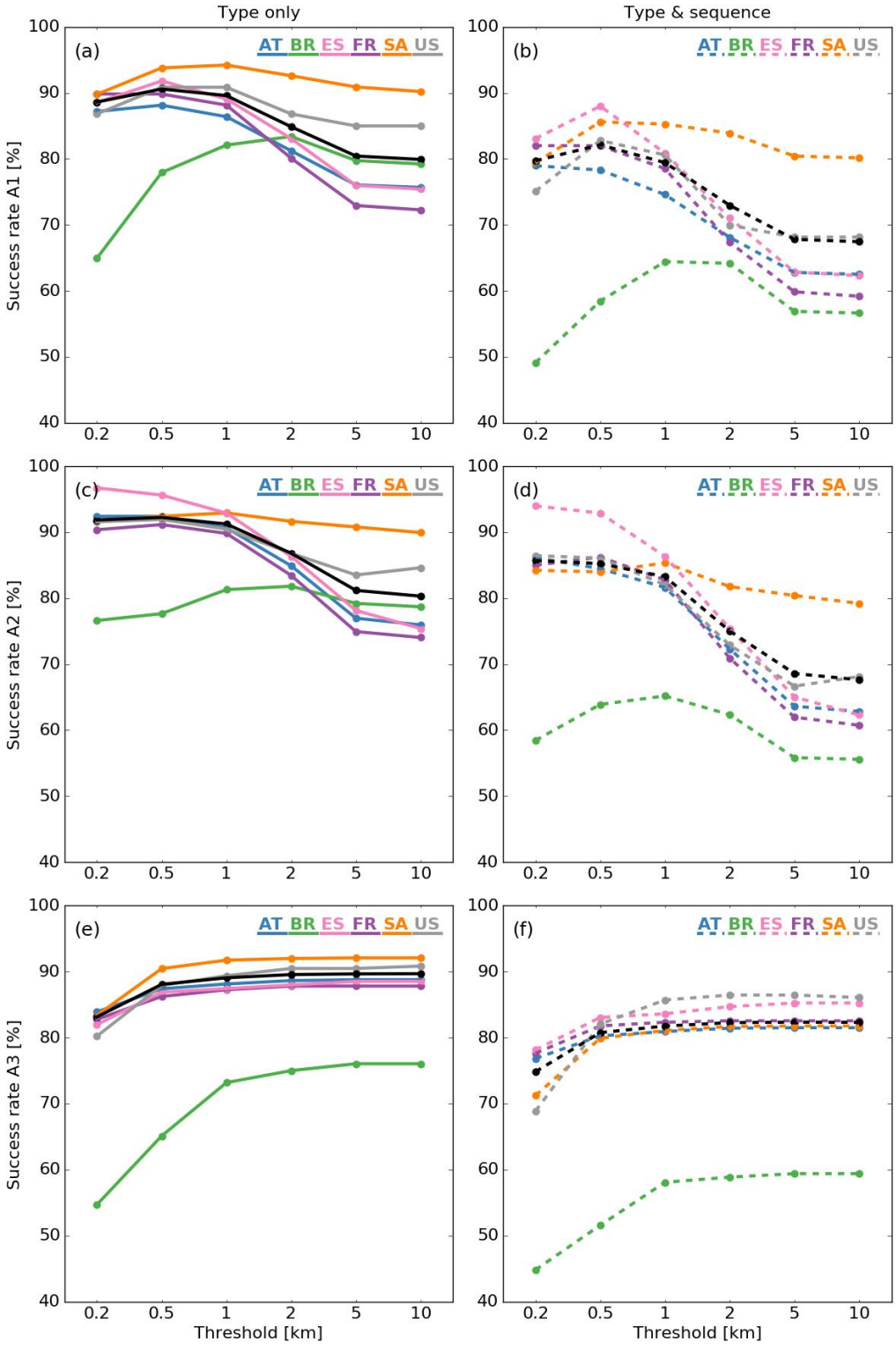

Figure 2: The success rate for the three algorithms is displayed in the "Type only" case (left plots) or the "Type and Sequence" (right plots) for algorithm A1 (a and b), A2 (c and d) and A3 (e and f). Colors are linked to each specific data set, whereas the black curve indicates the average result without Brazil.

https://doi.org/10.5194/nhess-2021-13
Preprint. Discussion started: 11 February 2021


Natural Hazards and Earth System Sciences Discussions

overlap with any of the other three. Depending on the adopted distance criterion, the algorithm results in either one or two GSPs.

5. Results

In the following analysis, a similar strategy is applied to all three algorithms. First of all, the ability to distinguish between a stroke creating a NGC and one that follows a PEC is examined. The latter will be denoted as the "Type only" criterion. Secondly, a stricter "Type and Sequence" criterion is validated. The latter not only checks whether the correct type is retrieved but additionally whether the order of occurrence is correct. By this it is meant that in the case of an NGC, whether it is correctly assigned as the 1st, 2nd, 3rd, … GSP in the flash, while in the case of a PEC, if it is assigned to the correct GSP as retrieved from the video images.

A1 and A3 have one obvious threshold in common, i.e., the distance to group strokes into a particular GSP. In the case of A2, only the low-SMA strokes are grouped according to a flash dependent distance threshold. However, to facilitate the comparison of the three algorithms, the plots on the left and right in Figure 2 display the probability of the algorithms to correctly assign the "Type only" and "Type and Sequence", respectively, of the strokes as a function of the distance threshold ranging from 200 meters up to 10 kilometers. The latter threshold is exactly the distance threshold used by A1 and A3, while in the case of A2 it is the threshold that subdivides the strokes into low- and high-SMA strokes, followed by the algorithms' specific designed distance threshold.

As will be demonstrated later on, the trend for AT, FR, SA, ES and US is similar for each specific algorithm, while BR exhibits a different behavior. It is believed that this behavior of BR is a consequence of the low LA of the LLS observations at that time, prohibiting the algorithm to utilize its full potential. For this reason, the overall success rate of the algorithms, as denoted by the black curve in Fig. 2, is calculated without taking into account BR. Results hereof are quantified in Table 2.

5.1. Results A1

The success rate in determining the type (and sequence) of the strokes is plotted in Figure 2a (2b). Although only better by one or two percent, the best overall "Type only" success rate of 90.6% is found adopting a distance threshold of 500 m. The algorithm displays a similar behavior for the "Type and Sequence" criterion, with an overall best of 82.1% at 500 m. Overall, a 10% to 15% drop is noticed if the sequence is additionally taken into account as criterion. In Table 2 the results for "Type only" are split into the classification success for NGC or PEC. Increasing the distance threshold in the algorithm leads to strokes being grouped more and more into a single GSP. As such, strokes are gradually more frequently allocated as a PEC by the algorithm. This explains the success rate of almost 100% for PEC at the largest threshold of 10km. Similar reasoning can explain the behavior of NGC, whereby NGC is better predicted than PEC at lower distance thresholds.

First strokes in the flash, including single stroke flashes, are per definition always correctly assigned by the algorithm. Hence, neglecting first strokes results in a decrease of the success rate by about 5% to 10%, indicated by the results between brackets in Table 2. On the other hand, neglecting first strokes does not affect the PEC classification.

https://doi.org/10.5194/nhess-2021-13
Preprint. Discussion started: 11 February 2021

Natural Hazards and Earth System Sciences Discussions

Table 2: Performance results for the three algorithms excluding BR, i.e., black curve in Fig. 2. Values in parenthesis are success rates for events without first strokes.

Distance threshold [km]	0.2	0.5	1	2	5	10
Algorithm 1						
Type only correct [%]						
All strokes	88.6 (82.4)	90.6 (85.8)	89.6 (84.3)	84.9 (77.1)	80.4 (70.3)	79.9 (69.5)
NGC	92.0 (79.0)	89.7 (72.5)	84.9 (58.9)	74.6 (30.5)	65.2 (4.4)	63.8 (0.8)
PEC	84.4	91.6	95.3	97.3	98.9	99.4
Type & Seq correct [%]						
All strokes	79.7 (69.2)	82.1 (72.9)	79.4 (68.8)	72.9 (58.8)	67.9 (50.8)	67.4 (50.3)
Algorithm 2						
Type only correct [%]						
All strokes	91.9 (87.5)	92.4 (88.0)	91.2 (86.5)	86.8 (79.7)	81.2 (71.0)	80.3 (69.6)
NGC	95.3 (87.1)	93.6 (82.3)	89.9 (71.8)	79.9 (44.0)	67.2 (8.6)	64.6 (1.3)
PEC	87.6	90.6	92.9	95.2	98.1	99.4
Type & Seq correct [%]						
All strokes	85.7 (78.0)	85.2 (77.3)	83.3 (74.2)	75.0 (61.5)	68.6 (51.6)	67.6 (50.1)
Algorithm 3						
Type only correct [%]						
All strokes	83.1 (74.0)	88.1 (81.6)	89.1 (83.1)	89.6 (83.9)	89.7 (84.1)	89.7 (84.1)
NGC	99.1 (97.5)	98.3 (95.4)	98.3 (95.2)	98.3 (95.2)	98.3 (95.2)	98.3 (95.2)
PEC	63.8	75.6	77.9	79.0	79.2	79.3
Type & Seq correct [%]						
All strokes	74.8 (61.2)	80.8 (70.3)	81.8 (71.9)	82.3 (72.7)	82.3 (72.8)	82.3 (72.8)

260

https://doi.org/10.5194/nhess-2021-13
Preprint. Discussion started: 11 February 2021


Natural Hazards and Earth System Sciences Discussions

The effect of not using the condition to group strokes with $|I_p|$ < 6kA and/or SMA > 2km in the previous GSP regardless of its location, results in a minor drop of the success rate by not more than 1 %. This is as expected since only a limited amount of strokes fall within this category.

Finally, it is worth mentioning that for an algorithm depending on solely a distance criterion to group strokes into GSPs, the success rate in the limit of very low and very high distance thresholds can be determined theoretically. This is true since all strokes will create a new GSP using the algorithm at very low distance thresholds while at very high distance thresholds, all strokes are grouped into a single GSP. Making use of the observed amount of flashes, strokes and GSPs, the success rate can then be determined at those boundary conditions. The average number of GSP per flash in the case of SA is lowest among the data sets, resulting in the best performance at high distance thresholds.

5.2. Results A2

The success rate in determining the type (and sequence) of the strokes is plotted in Figure 2c (2d). To reiterate, in the case of A2, the threshold displayed on the x-axis is the threshold that sorts strokes into low- and high-SMA strokes. As such, toward the left side of the plot some strokes will be regarded as large SMA strokes because the algorithm applies a combination of spherical grouping and elliptical scaling. On the other hand, at large distance thresholds, most of the strokes, if not all, are regarded as small SMA strokes and only spherical grouping is utilized. At a threshold of 10 km the outcome resembles the outcome of A1, due to the merging of the GSPs, if the distances are below 10 km. Hence, on this side of the plot most, if not all, flashes have one single GSP. At 200 m, the algorithm performs better for BR compared to the other two algorithms, a consequence of the elliptical scaling. In fact, the primary motivation behind implementing the hybrid scaling method used by this algorithm was to increase the performance in case of low sensor density networks or near borders. Hence, under the latter conditions the use of this algorithm is recommended. However, the success rate for BR remains low compared to the other data sets at low thresholds. Looking at Table 2, A2 performs best at the 500 m threshold with an overall “Type only” success rate being about 2 to 4 % higher than A1 and A3, respectively, and is similar in case of “Type and Sequence”.

5.3. Results A3

Figures 2e and 2f plot the success rate of correctly assigning the "Type only" and "Type and Sequence" in the case of A3. Compared to the previous two algorithms, the behavior exhibits a different pattern whereby the outcome for all data sets increases gradually up to a distance threshold of about 1km, after which the curve flattens out. Additionally, what is striking is that the results for the data sets are close to each other all over the line within approximately 5%, except for BR. The reason why an enlarged distance threshold has practically no effect beyond 1 km is the explicit condition that the 50% probability ellipse needs to overlap with one or more of the other error ellipses of strokes already assigned to the GSP. Hence, this prerequisite prevents grouping strokes located at large distances from each other into a single GSP, as opposed to A1, for example. One can conclude that for A3, the distance threshold dominates when assigning a stroke to a GSP or to create a NGC at thresholds smaller than the average SMA values observed in Table 1, whereas the SMA values quickly

https://doi.org/10.5194/nhess-2021-13
Preprint. Discussion started: 11 February 2021

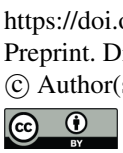

Natural Hazards and Earth System Sciences
Discussions

become more important at larger distance thresholds. This is true, since for large thresholds it can be assumed that all strokes are within the threshold distance. The decision to group these into a GSP is determined by whether the ellipses overlap or not. Similar to A1 and A2, the data for BR exhibits the worst probability of success.

The results for the black curve in Fig. 2e and 2f are quantified in Table 2. A somewhat smaller drop than 10% in the success rate is observed going from "Type only" to "Type and Sequence". A more detailed look at the classification success of NGC and PEC reveals that the behavior is different when compared to the other algorithms. Here, NGC's classification success is rather stable over the entire line. Moreover, excluding first strokes does not have such a dramatic effect on the outcome as opposed to A1 and A2.

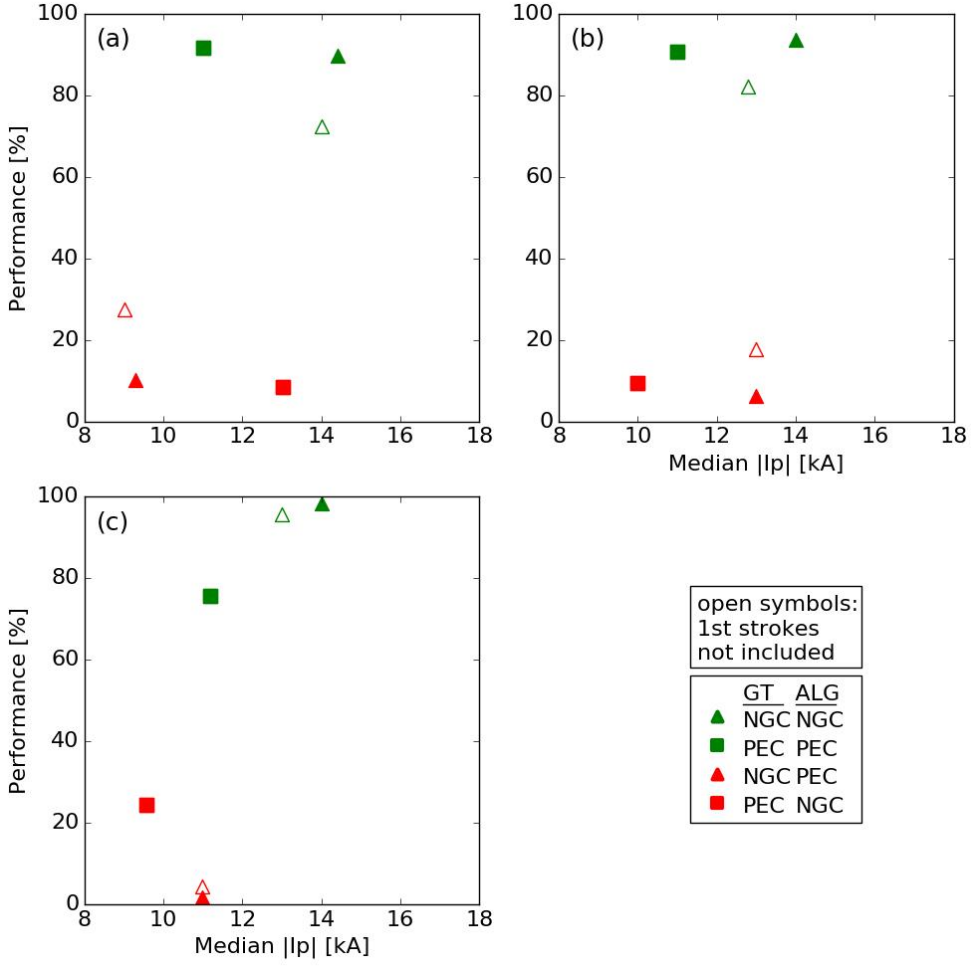

Figure 3: Algorithm performance as a function of median absolute peak current for (a) A1, (b) A2, and (c) A3. The threshold for which the results are presented is 500m for A1 and A2, and 10km for A3. The different symbols and colors denote the four possibilities, whereby a green (/red) color indicate that the algorithm (ALG) correctly (/incorrectly) assigned the type of the stroke compared to the ground-truth observations (GT). Ignoring first strokes in the flash results in the open symbols in the plots.

https://doi.org/10.5194/nhess-2021-13
Preprint. Discussion started: 11 February 2021


Natural Hazards and Earth System Sciences Discussions

5.4. Dependence on the estimated peak current

Figure 3 plots the overall performance of the algorithm to determine the type of the strokes as a function of the median absolute peak current I_p. The results are presented, adopting the threshold of 500 m for all three algorithms. A different symbol and color is used for each of the four possible combinations, with open symbols denoting the results when first strokes are neglected.

For all the algorithms, the correctly assigned NGC strokes (green triangles) have a median $|I_p|$ that is larger compared to the incorrectly assigned ones (red triangles). This difference is more pronounced in the case of A1 and A3, while it is only 1 kA for A2. The smaller difference in median $|I_p|$ between the correctly and incorrectly assigned NGC strokes in case of A2 indicates that the correct classification is less dependent on the stroke's peak current compared to the other two algorithms. The effect of neglecting the first strokes (open symbols) has been discussed before. A drop is noticed in the success rate of the algorithms according to the results listed in Table 2 (open triangles). While for A1 and A3, a similar behavior is found in terms of the median peak currents, for A2 it is found that the absolute median Ip for incorrectly assigned NGCs is slightly larger by 0.5 kA as compared to the correctly assigned ones.

Similarly, one can look at the peak currents of the PECs. In the case of A2 and A3, correctly assigned PECs (green squares) have larger absolute median I_p compared to the incorrectly assigned ones (red squares), whereas the opposite is found for A1. The performance of A1 related to PECs is a consequence of assigning strokes with an absolute peak current below 6 kA (and/or SMA value larger than 2 km) to the previous GSP regardless of its position. As such, those particular low peak current strokes reduce the median peak current of correctly assigned PEC strokes in Fig. 3a.

6. Conclusions

Three different ground strike point algorithms have been assessed in terms of their ability to correctly group strokes into ground strike points. The input for the algorithms is provided by the observations made by local LLSs, whereas high-speed observations deliver the ground-truth observations against which the outcome of the algorithms are tested. Although some differences are noticeable among the algorithms, all three of them perform well with success rates up to 90% to retrieve the correct type of strokes in the flash. This means that in 90% of the cases, the number of ground strike points are retrieved as how they actually occurred in nature.

All three algorithms, with their proper characteristics, are high-performance tools both in speed and accuracy to group strokes into ground strike points. It is difficult to favor one algorithm over the other. In absolute terms, A2 performs the best, but only by a few percent. However, it is also the most complicated algorithm among the three, combining spherical grouping and elliptical scaling. The other two algorithms either solely depend on a distance and/or overlap of the error ellipses and are more straightfoward to implement by the user.

In the end, the quality of the local LLS is of particular importance in the success rate of the algorithm.

https://doi.org/10.5194/nhess-2021-13
Preprint. Discussion started: 11 February 2021


Natural Hazards and Earth System Sciences Discussions

Acknowledgments

The authors would like to thank the South African Weather Services (SAWS) for use of the SALDN data, specifically Mr Morné Gijben, Andrew van der Merwe and Michelle Hartslief. The authors would like to thank Mr Tom Warner and Dr Carina Schumann for use of the South African high-speed video footage as ground-truth data. Additionally, the efforts of C. Mata for the USA data set and of X. Delorme, J. B. Varela, A. R. Espana for the ground-truth data taken in France and Spain are highly appreciated. Special thanks go to H. Kohlmann who helped DRP with QGis to correctly plot the error ellipses in appropriate projections used throughout this study. The authors would like to thank the National Research Foundation of South Africa (Unique Grant No: 98244).

References

Ballarotti, M. G., Saba, M. M. F., and O. Pinto Jr.: A new perfomance evaluation of the Brazilian Lightning Location System (RINDAT) based on high-speed camera observations of natural negative ground flashes. proc. 19th Int. Lightning Detection Conf. (ILDC), Tucson, Az, Vaisala, 2006.

Biagi, C. J., Cummins, K. L., Kehoe, K. E., and Krider, E. P.: National Lightning Detection Network (NLDN) performance in southern Arizona, Texas, and Oklahoma in 2003–2004. J. Geophys. Res., 112, D05208, https://doi.org/10.1029/2006JD007341, 2007.

Campos, L. Z. S., Cummins, K. L., and Pinto Jr. O.: An algorithm for identifying ground strike points from return stroke data provided by lightning location systems, Asia-Pacific Conference on Lightning (APL), Nagoya, Japan, 2015

Campos, L. Z. S.: On the mechanisms that lead to multiple ground contacts in lightning, Doctorate Thesis of the Graduate Course in Space Geophysics, Instituto Nacional de Pesquisas eEpaciais (INPE), http://urlib.net/8JMKD3MGP3W34P/3LG4CDL, Chapter 4, 2016.

Cramer, J. A., and Cummins, K. L.: Evaluating location accuracy of lightning location networks using tall towers. 23rd Int. Lightning Detection Conf., Tucson, AZ, Vaisala, 2014.

Cummins, K. L., Zhang, D., Quick M. G., Garolera, A. C., and Myers, J.: Performance of the US NLDN during the Kansas Windfarm 2012 and 2013 field programs. 23rd Int. Lightning Detection Conf., Tucson, AZ, Vaisala, 2014.

Cummins, K. L.: Analysis of multiple ground contacts in cloud-to-ground flashes using LLS data: the impact of complext terrain, 22nd International Lightning Detection Conference, Broomfield, Colorado, USA, 2-3 April, 2012.

Diendorfer G., A review of 25 years of lightning research in Austria from 1991-2015, World meeting on Lightning, 2016.

Fensham, H.G., Schumann, C., Hunt, H.G.P., Nixon, K.J., Warner, T.A., Gijben M., Performance evaluation of the SALDN using high- speed camera footage of ground truth lightning events over Johannesburg, South Africa, 34th International Conference on Lightning Protection (ICLP), Rzeszow, Poland, 2018.

Gijben, M.: Lightning Climatology of South Africa – South African Journal of Science, Vol 108, No 3/4. http://dx.doi.org/10.4102/sajs.v108i3/4.740, 2012.

https://doi.org/10.5194/nhess-2021-13
Preprint. Discussion started: 11 February 2021


Natural Hazards and Earth System Sciences Discussions

Hermant, A.: Traqueur d'Orages. Les rendez-vous de la nature, ISSN 1285-9168, Publisher: Nathan, 2000, ISBN: 2092605461, 9782092605462, 2000.

Hunt, H.G.P., Liu, Y. C. and Nixon, K.: Evaluation of the South African Lightning Detection Network using photographed tall tower lightning events from 2009-2013, 32rd International Conference on Lightning Protection (ICLP), Shanghai, China, 2014.

Hunt, H.G.P, Nixon, K.J., Jandrell, I.R., Schulz, W.: Can we model the statistical distribution of lightning location system errors better?, Electric Power Systems Research Journal 178, 2020.

Jerauld, J., Rakov, V. A., Uman, M. A., Ramb,o K. J., Jordan, D. M., Cummins, K. L., and Crame,r J. A.: An evaluation of the performance characteristics of the US National Lightning Detection Network in Florida using rocket-triggered lightning. J. Geophys. Res., 110, D19106, https://doi.org/10.1029/2005JD005924, 2005.

Lafkovici, A., Hussein, A. M., Janischewskyj, W., and Cummins, K. L.: Performance analysis of the North American Lightning Detection Network using CN Tower lightning data. 19th Int. Lightning Detection Conf., Tucson, AZ, Vaisala, 2006.

Mallick, S., and Coauthors: Performance characteristics of the NLDN for return strokes and pulses superimposed on steady currents, based on rocket-triggered lightning data acquired in Florida in 2004–2012. J. Geophys. Res. Atmos., 119,3825–3856, https://doi.org/10.1002/2013JD021401, 2014.

Matsui, M., Michishita, K., and Yokoyama, S.: Characteristics of negative flashes with multiple ground strike points located by the Japanese lightning detection network, in IEEE Transactions on Electromagnetic Compatibility, vol. 61, no. 3, pp. 751-758, doi: 10.1109/TEMC.2019.2913661, 2019.

Naccarato, K. P., and O. Pinto Jr.: Improvements in the detection efficiency model for the Brazilian lightning detection network (Brasil- DAT), Atmos. Res., 91, 546–563, doi:10.1016/j.atmosres.2008.06.019, 2009.

Nag, A., Murph,y M. J., Cummins, K. L., A. E. Pifer, and J. A. Cramer: Recent evolution of the US National lightning Detection Network. 23rd Int. Lightning Detection Conf., Tucson, AZ, Vaisala, 2014.

Nag, A., and Coauthors: Evaluation of US National Lightning Detection Network performance characteristics using rockettriggered lightning data acquired in 2004–2009. J. Geophys. Res., 116, D02123, https://doi.org/10.1029/2010JD014929, 2011.

Pedeboy, S.: Identification of the multiple ground contacts flashes with lightning location systems, CIGRE C4 Colloquium on Power Quality and Lightning, Sarajevo, Bosnia and Herzegovina, 13-16 May, 2012.

Poelman, D. R., Schulz, W., Diendorfer, G., and Bernardi, M., the European lightning location system EUCLID – part 2: observations, Nat. Hazards Earth Syst. Sci. 16 (2), 607-616, 2016.

Schulz, W., Pichler, H., and Diendorfer, G.: Evaluation of 45 negative flashes based on E-field measurements, video data and lightning location data in Austria. Proc. 30th Int. Conf. on Lightning Protection, Cagliari, Italy, Power and Energy Society, 1011-1–1014, 2010.

https://doi.org/10.5194/nhess-2021-13
Preprint. Discussion started: 11 February 2021


Natural Hazards and Earth System Sciences Discussions

Schulz, W., Diendorfer, G., Pedeboy, S., and Poelman, D. R.: The European lightning location system EUCLID – Part 1: Performance analysis and validation. Natural Hazards and Earth System Sciences, 16(2), 595–605. https://doi.org/10.5194/nhess-16-595-2016, 2016.

Stall, C. A., Cummins, K. L., Krider, E. P., and Cramer, J. A.: Detecting Multiple Ground Contacts in Cloudto-Ground Lightning Flashes, Journal of Atmospheric and Oceanic Technology, 26(11), 2392-2402, 2009.

Thottappillil R., Rakov, V. A., Uman, M. A., Beasley, W. H., Master, M. J., and Shelukhin, D. V., Lightning subsequent-strokeelectric-field peak greater than the 1st stroke peak and multiple ground terminations, Journal of Geophysical Research-Atmospheres, 97(D7), 7503-7509, 1992.

Valine, W. C., and Krider, E. P.: Statistics and characteristics of cloud-to-ground lightning with multiple ground contacts, Journal of Geophysical Research-Atmospheres, 107(D20), 2002.

Zhang, D., Cummins, K. L. and Nag, A.: Assessment of cloud lightning detection by the US National Lightning Detection Network using video and Lightning Mapping Array observations. Seventh Conf. on the Meteorological Applications of Lightning Data, Phoenix, AZ, Amer. Meteor. Soc., 7.1, https://ams.confex.com/ams/95Annual/webprogram/Paper262568.html., 2015.